(Received 14 September 2023, Accepted 5 April 2024, Scheduled 16 April 2024)

Optimizable KNN and ANFIS Algorithms Development for Accurate Antenna Parameter Estimation

Rajendran Ramasamy* and Maria Anto Bennet

Department of Electronics and Communication Engineering
Vel Tech Rangarajan Dr. Sagunthala R&D Institute of Science and Technology, Chennai 600062, India

ABSTRACT: The process of smart antenna synthesis involves the automatic selection of the optimal antenna type and geometry in order to enhance antenna performance. A model for intelligent antenna selection employs an optimizable K-nearest neighbors (KNN) classifier to determine the optimal antenna choice. To optimize the utilization of different learner types, the geometric parameters of the antenna are presented as the final step prior to the construction of the Adaptive Neuro-Fuzzy Inference System (ANFIS) model, which involves the integration of five distinct primary learners. The classification of three distinct types of antennas, namely helical antenna, pyramidal horn antenna, and rectangular patch antenna, is performed using an optimizable K-nearest neighbors (KNN) classifier. Additionally, an ANFIS approach is employed to determine the optimal size parameters for each antenna. The accuracy is used to evaluate the performance of an optimizable KNN classifier, whereas Mean Squared Error and Mean Absolute Percentage Error are used to evaluate the performance of an ANFIS. The proposed technique demonstrates high performance in parameter prediction and antenna categorization, achieving a Mean Absolute Percentage Error of less than 3% and an accuracy exceeding 99.16%. The recommended methodology holds significant potential for widespread application in the development of practical smart antennas.

1. INTRODUCTION

ANFIS is a sophisticated combination system that addresses complicated problems by combining the principles of fuzzy logic and neural networks. The utilization of ANFIS extends beyond its common applications in regression and optimization tasks, as it can also be employed to address antenna classification problems. The process of antenna classification involves categorizing different types of antennas based on specific attributes, such as their radiation pattern, frequency range, polarization, and structural characteristics. ANFIS can be employed to develop a classification model that effectively and autonomously categorizes antenna types by acquiring knowledge of the associations between input variables and antenna types. Antennas play a crucial role in the functioning of consumer electronics, necessitating the development of more precise and efficient designs. Pujara et al. proposed an optimization algorithm for Horn antenna using ANFIS, aiming to enhance the accuracy of parameter estimation. Several ANFIS models were developed in order to enhance computational speed while maintaining accuracy [1, 2]. Kapetanakis et al. proposed an algorithm for optimizing the parameters of a circular loop antenna using artificial intelligence and fuzzy logic techniques, with the aim of achieving efficient parameter estimation. The researchers devised neural network learning techniques that exhibited exceptional accuracy, rapid convergence, and efficient computational performance [3].

This paper presents a novel approach for evaluating the effectiveness of a resonant frequency through the utilization of an Adaptive Neuro-Fuzzy Inference System (ANFIS) in the design of a single-layer patch antenna. The ANFIS method that has been proposed exhibits a low Mean Absolute Percentage Error (MAPE), a high level of accuracy, and demonstrates a reduced computational time [4, 5]. Kayabasi proposed the utilization of neuro fuzzy-based triangular patch antennas for the purpose of determining the operational frequency of the aforementioned antenna [6]. Yahya et al. suggested a C-shaped microstrip patch antenna by contrasting several regression methods. A machine learning model named PQGR was developed, which demonstrates the ability to reduce error rates in addition to minimizing metrics such as maximum entropy (ME), mean square error (MSE), root-mean-square error (RMSE), and average percentage error (APE) [7, 8]. This study employs a K-nearest neighbors (KNN) based estimator to ascertain the operating frequencies of slot antennas. The KNN method, as proposed, demonstrates a notable level of accuracy while requiring a reduced amount of computational time [9]. The present study introduces a novel computational analytical approach that utilizes a surrogate model to estimate antenna parameters, specifically the resonant frequency and bandwidth. The authors developed the Particle Swarm Optimization (PSO) and Differential Evolution (DE) algorithms, which have the capability to enhance computational efficiency while maintaining a high level of accuracy [10, 11]. Hu et al. proposed the use of VHF and UHF helical antennas for satellite communications. Their research demonstrated that the suggested helical antenna design achieved significant beam coverage [12]. Maged et al. designed

* Corresponding author: Rajendran Ramasamy (rramasamy2014@gmail.com).

helical antennas for satellite applications with improved gain. They created a truncated horn using an optimization technique involving genetic algorithms [13]. An enhanced version of helicone antennas was suggested by Sadeghikia et al. Taking size and mass constraints into account necessitates optimization in order to attain maximum gain [14]. Falkner et al. proposed a methodology for parameter estimation that enhances effectiveness, utilizing an automated machine learning technique, within the context of optimizing a travelling wave antenna. An automated machine learning method was developed for the purpose of calculating return loss and gain [15, 16]. Moshtaghzadeh et al. proposed a methodology rooted in machine learning to optimize the parameter estimation of a foldable origami helical antenna, aiming to enhance its effectiveness. The authors developed Finite Element Method (FEM) and Artificial Neural Network (ANN) techniques, which exhibit high precision and computational efficiency as evidenced by previous studies [17, 18]. Polo-López et al. proposed an optimization algorithm for horn antennas based on genetic algorithms. Fruit fly optimization algorithm (FOA) was developed and introduced as an optimization tool specifically designed for challenging antenna designs, demonstrating a high degree of accuracy [19]. The integration of the PSO algorithm with the Gaussian process is employed in this study to enhance the efficiency of antenna design optimization [20].

As a result, calculation times may be shortened without compromising accuracy and efficiency. This paper introduces the Thompson sampling efficient multiobjective optimization (TSEMO) approach, which aims to optimize antennas effectively. The proposed method utilizes a deep neural network (DNN) framework. The proposed optimization method is effectively utilized by designers as a means of resolving complexity and high structure dimensions in the field of antenna design [21–23]. The method proposed in this study demonstrates significantly improved computational efficiency compared to traditional machine learning techniques, such as ANN and Bayesian optimization. By reducing the size of the data sets required for analysis, the method achieves a speed enhancement ranging from 5 to 30 times faster, as demonstrated by previous research [24–26]. This study introduces various methods for optimizing antennas using genetic algorithms. The installation process of this system is straightforward due to its compact size [26–30]. This research presents a slot microstrip antenna based on ANN for the evaluation of parameters such as S_{11}, gain, voltage standing wave ratio (VSWR), and efficiency [31]. Based on the comprehensive literature review outlined previously, it was observed that a number of studies have proposed machine learning models that effectively classify antenna types. However, there is a limited amount of research that has focused on estimating the parameters of an antenna following its classification. Furthermore, compromises were made with respect to the speed of computation, although there is still room for improvement in terms of the accuracy of parameter estimates. The proposed technique, referred to as Optimizable KNN+ANFIS, demonstrates a high level of accuracy in predicting antenna parameters by employing ANFIS and leveraging Optimizable KNN for the purpose of categorizing three distinct types of radiating element: microstrip radiating element, horn radiating element, and helical radiating element. The ANFIS demonstrates a high level of precision and efficiency in estimating the dimensions of various types of antennas, such as the width of microstrip patch antennas, the diameter of helical antennas, and the diameter of horn antennas. The ANFIS enables the comprehensive analysis of intricate relationships between features and labels, thereby augmenting the modeling adaptability for intricate antenna characteristics. In contrast, Optimizable KNN is a technique that offers simplicity and efficiency in computational processes, particularly when dealing with datasets of moderate size.

2. SYSTEM DESCRIPTION

Figure 1 illustrates the intelligent antenna synthesis system that is recommended. The framework of the proposed system comprises two main components, namely ANFIS model and intelligent classification module.

The antenna characteristics such as reflection coefficient (S_{11}), resonant frequency (f_r), gain (G), and bandwidth (BW) are input into a K-nearest neighbors (KNN) classification model that has been trained effectively. This model is utilized to classify the antenna type that is most appropriate for the initial step of the system. The subsequent elaboration of the optimal antenna parameter design is accomplished through the utilization of the ANFIS technique. The initial step involves examining the impact of the antenna's properties on the overall model's performance through the utilization of the switch variate approach. Because each antenna has numerous parameter sets, simulating different values for each parameter would result in an excessively large dataset and significant use of computational resources. The analytical formulas found in the existing scholarly literature are employed to ascertain the factors that have a substantial impact on the results of each type of antenna. Subsequently, the HFSS toolbox is employed to generate electromagnetic simulation outcomes that align with the aforementioned variables. The optimizable KNN algorithm is a supervised learning classification technique that aims to predict the accurate classification of a novel sample by utilizing a set of data points or vectors that have been categorized into different classes. A robust classification model is developed through iterative training of an optimizable K-nearest neighbors (KNN) algorithm using cross-validation techniques, and by integrating diverse datasets containing different antenna configurations. Optimizable KNN classifiers are effectively employed in diverse domains. The primary characteristic that distinguishes them is their proficiency in deriving informative decision-making insights from the available data. It is feasible to generate an optimizable KNN model from training sets for different antenna configurations. When the optimizable KNN classifier accurately predicts the antenna, the output value for the specific class is assigned as one, while the output values for the remaining classes are assigned as zero. The ANFIS is activated exclusively when both inputs exhibit identical values, and the output of the optimizable KNN classifier is subsequently supplied to an AND gate. The ANFIS framework maintains datasets that encompass the specifications of optimal antenna size parameters corresponding to the input design

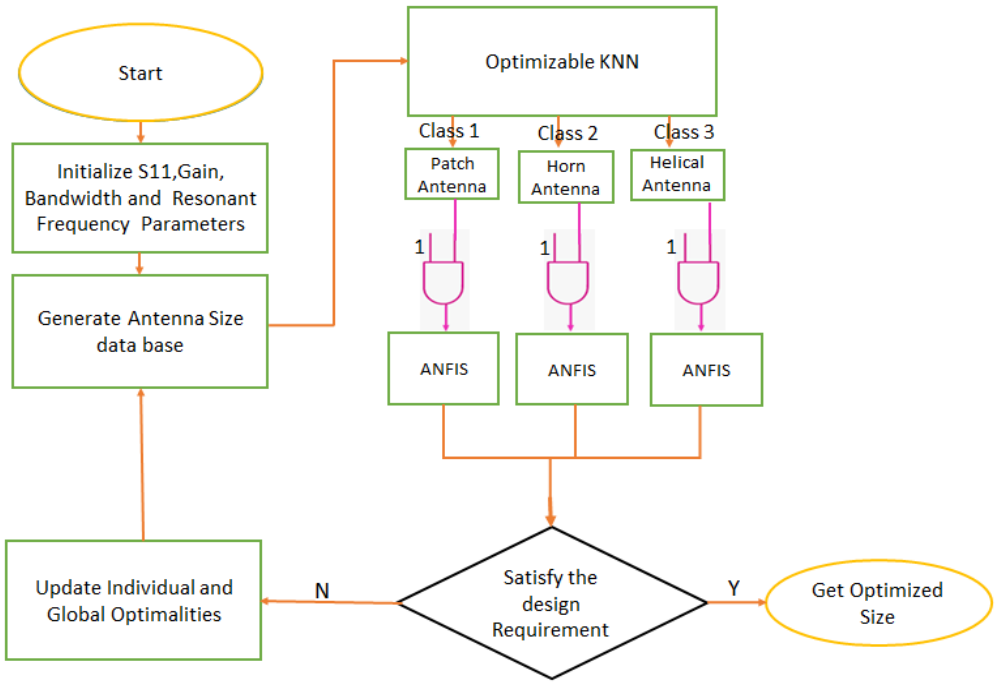

FIGURE 1. Proposed intelligent antenna synthesis system.

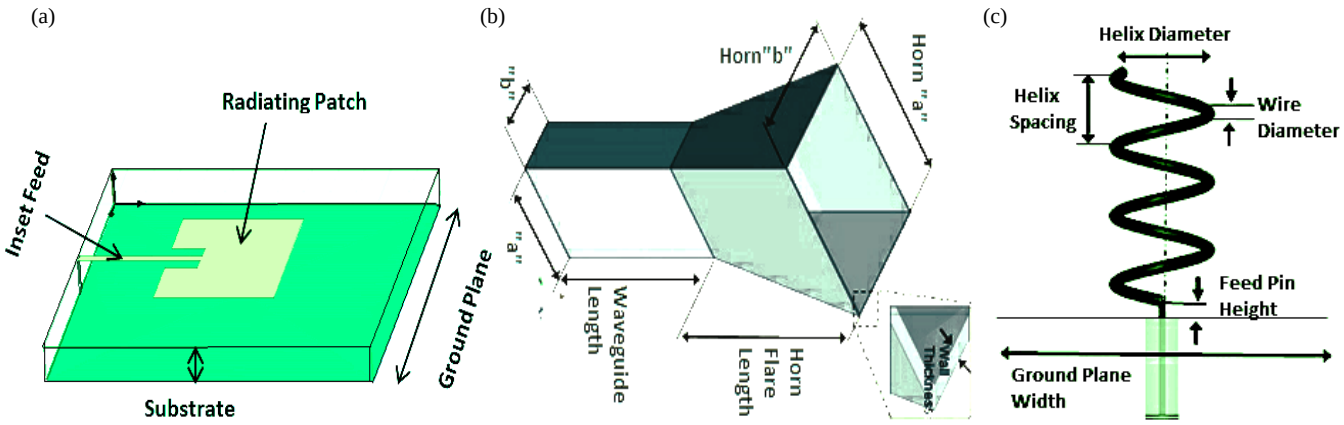

FIGURE 2. (a) Proposed microstrip antenna. (b) Proposed horn antenna. (c) Proposed helical antennas.

parameters, including S_{11}, resonant frequency, bandwidth, and gain. Once the ANFIS has been assessed using a specific set of design parameters and compared to preexisting datasets, the outcomes pertaining to the optimal antenna size parameters are subsequently provided.

3. METHODS DESCRIPTION

3.1. Proposed Antenna

The patch antenna comprises three main components, namely the radiating element, substrate, and ground plane, as depicted in Figure 2(a). These components exhibit various geometric parameters, including width of the patch and length of the patch, which contribute to the antenna's overall design and performance. The input parameters of a microstrip patch antenna include values for S_{11}, gain, bandwidth, and resonant frequency. The output parameter of the microstrip patch antenna is the width. The resonant frequency exhibits a range spanning from 2.4 GHz to 5 GHz, as indicated in the accompanying table. The values were derived from the HFSS toolbox. The technique proposed in our study utilizes microstrip patch antenna parameters to estimate various parameters by employing an optimizable KNN classifier and ANFIS technology. The data is obtained through simulation using the HFSS toolbox.

Rectangular patches are the most frequently utilized type. The investigation of the transmission line and cavity models, which exhibit enhanced accuracy when being applied to thin substrates, does not pose significant challenges. The structural layout of the pyramidal horn antenna is illustrated in Figure 2(b). The pyramidal horn antenna possesses various geometrical characteristics, including but not limited to the horn diameter (h_d), horn length (h_l), thickness of the wall, length

TABLE 1. Corresponding ranges of the antenna performance parameters.

Performance Parameters	Helical Antenna	Microstrip Patch Antenna	Pyramidal Horn Antenna
Reflection Coefficient (dB)	$-12.5 \sim -18$	$-14 \sim -39$	$-17 \sim -27$
Resonant Frequency (GHz)	$1.1 \sim 6.9$	$2.5 \sim 5$	$3.1 \sim 28$
Bandwidth (GHz)	$0.45 \sim 2.1$	$0.0555 \sim 0.1041$	$0.205 \sim 0.3483$
Gain (dB)	$11.2 \sim 14.8$	$5.1 \sim 8$	$1.1 \sim 28.9$

of the waveguide, and flare length of the horn. The pyramidal horn is a geometric shape commonly used in antenna design and acoustics. The proposed technique utilizes antenna parameters to estimate various parameters through the application of an optimizable KNN classifier and ANFIS technology. The computation of the gain of a horn antenna is facilitated by its design factors, which include axial length, path difference, flare angle, and aperture dimension. These parameters contribute to the overall simplicity of the gain calculation process for the horn antenna. Pyramidal horns are designed with the purpose of facilitating high gain. The structural layout of the helical antenna is depicted in Figure 2(c). The geometrical characteristics of this antenna include helix diameter (h_d), wire diameter (w_d), ground plane width, and feed pen height. Helical antennas are considered to be the primary type of antennas utilized in ultra-high frequency applications. The input parameters for a helical antenna include S_{11}, gain, bandwidth, and resonant frequency values. The output parameter for a helical antenna is the helix diameter. The resonant frequency exhibits a range spanning from 1 gigahertz (GHz) to 6 gigahertz (GHz), as indicated in the accompanying table. The values were derived using the HFSS toolbox. The technique proposed in our study utilizes helical antenna parameters to estimate various parameters through the application of an optimizable KNN classifier and ANFIS technology. The data is obtained through simulation using the HFSS toolbox.

3.2. Dataset

The selection of the microstrip patch antenna with compact dimensions is primarily based on the overall characteristics exhibited by patch antennas, such as the wide bandwidth of the helical radiating element and the high gain of the pyramidal horn radiating element. Table 1 displays the pertinent intervals for the parameters pertaining to the performance of the antenna. The selection of the geometric parameter for the rectangular patch antenna in Section 3 is based on theoretical investigation, specifically the patch width (w). The parameter variable for the pyramidal horn antenna is denoted as the diameter of the horn (d). Furthermore, the selection of helix diameter (h_d) was made as the geometric parameter for a helical antenna. The data is derived using the HFSS toolbox simulation. The width parameters of the microstrip patch antenna range from 13.75 to 29.42 mm. The pyramidal horn radiating element exhibits a range of horn diameters, spanning from 4 to 10 cm. The helical antenna exhibits a range of 1.59–9.541 cm for its diameter. Each individual antenna produces a collective sum of 50 data points, of which 80% are allocated for the purpose of training and validating the optimizable KNN and ANFIS models. The remaining 20% of the data is reserved for evaluating the performance of the models.

3.3. Optimizable KNN Classifier

The proposed methodology consists of three distinct categories: category A, which pertains to microstrip patch antennas; category B, which pertains to horn antennas; and category C, which pertains to helical antennas. Additionally, a new data point, denoted as x1, will be assigned to one of these categories. A K-nearest neighbors (KNN) algorithm that can be optimized was proposed as a solution for addressing this particular issue. The optimizable KNN algorithm enables efficient determination of the category or class of a given dataset. Figure 3 illustrates the flowchart representing the optimizable KNN classifier. Figures 4(a) and 4(b) show the effect of optimization on the KNN algorithm before and after optimization.

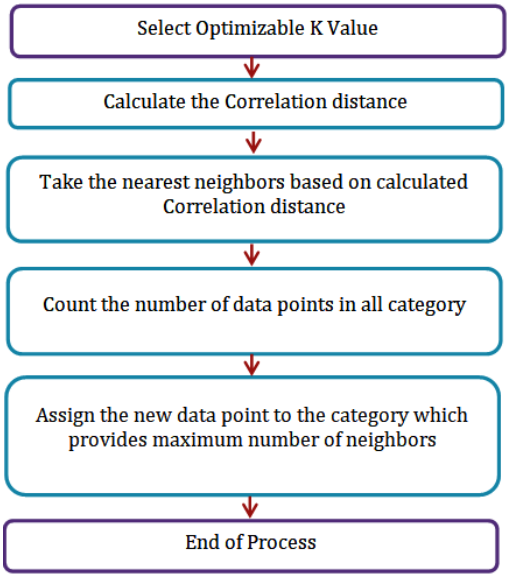

FIGURE 3. Flow chart for optimizable KNN classifier.

3.4. Optimizable on KNN Algorithm

Step-1 Choose the number K of neighbours.

Step-2 Determine the correlation distance between K neighbours.

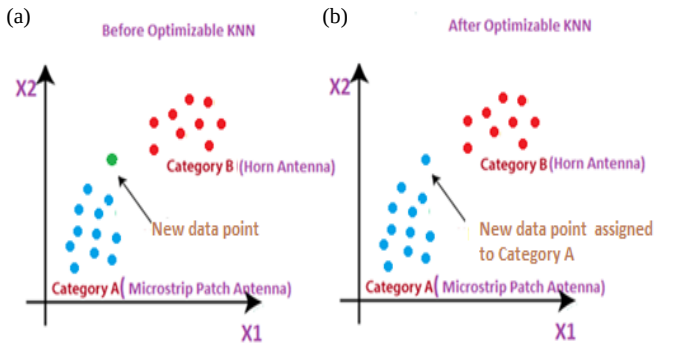

FIGURE 4. Effect of optimization on KNN algorithm. (a) KNN algorithm before optimization. (b) KNN algorithm after optimization.

Correlation distance between antenna A_1 and antenna B_1 is represented as

$$d_{st} = 1 - \frac{(X_s - \check{X}_s)(Y_t - \check{Y}_t)'}{\sqrt{(X_s - \check{X}_s)(X_s - \check{X}_s)'}\sqrt{(Y_t - \check{Y}_t)(Y_t - \check{Y}_t)'}} \tag{1}$$

where $\check{X}_s = \frac{1}{n}\sum_j X_{sj}$ and $\check{Y}_t = \frac{1}{n}\sum_j Y_{tj}$.

Step-3 Based on the optimal Correlation distance, select the optimized K nearest neighbour value.

Step-4 Count how many data elements there are in each group among these opmizable K neighbours.

Step-5 Assign the additional data points to the category where the neighbour count is at its highest.

Step-6 Our model is complete.

3.5. ANFIS Architecture

Adaptive Neuro-Fuzzy Inference System (ANFIS) employs learning algorithms to simulate and analyze the mapping relationship between input and output data in order to optimize the settings of a Fuzzy Inference System (FIS).

The ANFIS architecture is composed of several layers, including an input layer, an input membership function layer, a rule layer, an output membership function layer, and an output summation layer. The architecture of the ANFIS is depicted in Figure 5. The ANFIS model is founded upon the principles of the Sugeno fuzzy model. P_k is represented as.

$$P_k: \text{ IF } \mu X_i(a) \text{ AND } \mu Y_i(b) \text{ THEN } h = c_k + d_k + e_k \tag{2}$$

k — Number of regulations.

In the rule's antecedent component, fuzzy membership functions X_i and Y_i are indicated by μ. P_k, c_k, d_k, and e_k are the linear parameters of the kth rule's consequent component.

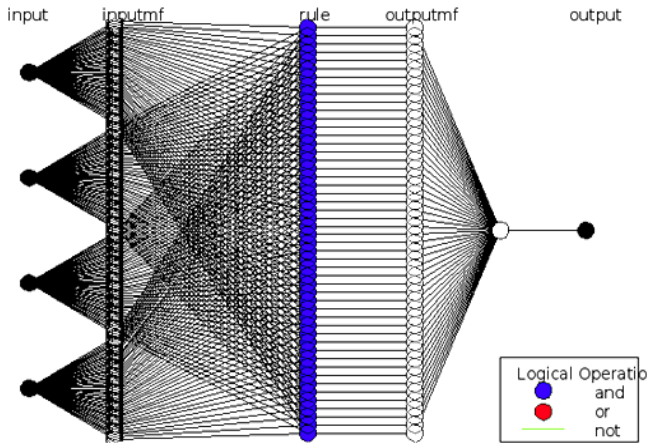

FIGURE 5. Architecture of ANFIS.

Layer 1 (Input layer)

Each node in this layer possesses a node membership function that is adaptive.

$$\mu X_i(a), \quad i = 1, 2, ..., 50 \tag{3}$$

$$M_i^2 = \mu Y_i(b), \quad i = 1, 2, ..., 50 \tag{4}$$

In our proposed methodology triangular shape fuzzy member function is used.

Layer 2 (Input membership function)

Determine the rule view product operation's firing strength.

$$M_i^2 = \overline{w_i} = \mu X_i(a) * \mu Y_i(b), \quad i = 1, 2, ..., 50 \tag{5}$$

Layer 3 (Fuzzy rules)

Determine a rule's normalised firing strength from a preceding layer.

$$M_i^3 = \overline{w_i} = \frac{w_i}{\sum w_i}, \quad i = 1, 2, ..., 50 \tag{6}$$

Layer 4 (Output membership function)

Each node in a fuzzy rule specifies the subsequent component. The rule consequent's sequential weights can be trained.

$$M_i^4 = \overline{w_i} \cdot h_i = \overline{w_i} \cdot (c_k x + d_k y + e_k), \quad i =, 2, ..., 50 \tag{7}$$

c_k, d_k, e_k are the sequential weights. In the preceding equation, x and y represent the input and output variables.

Layer 5 (Summation layer (or) output layer)

By adding the outputs of all the rules, nodes in layer 5 defuzzify the subsequent section of the rules.

$$M_i^5 = \sum_{i=1}^{n} \overline{w_i} \cdot h_i = \sum_{i=1}^{n} \overline{w_i} \cdot (c_k x + d_k y + e_k) \tag{8}$$

ANFIS can process precise input. Membership functions and fuzzy rules are used to represent various antenna parameters such as S_{11}, gain, frequency, and bandwidth, and fuzzy rules are again used to create clear output for logical purposes. The variables x and y in the above equation denote input and output, respectively.

4. RESULT AND DISCUSSION

The utilization of a confusion matrix serves as a method for effectively representing the performance evaluation of antenna classification. The term "matching matrix" is synonymous with

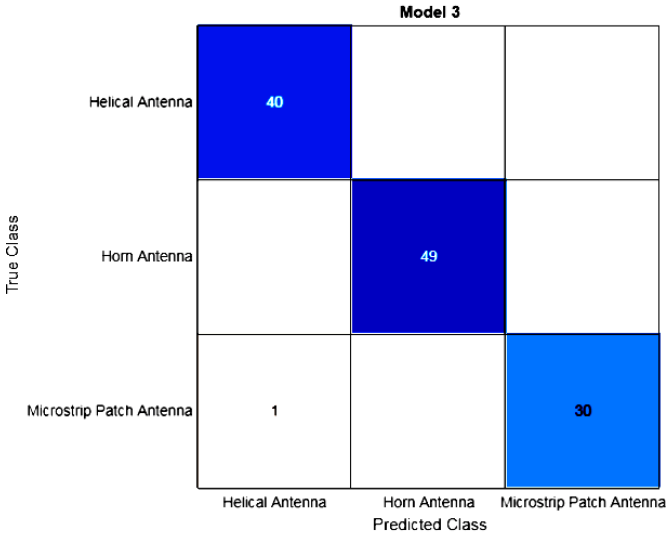

FIGURE 6. Confusion matrix of the antenna classification.

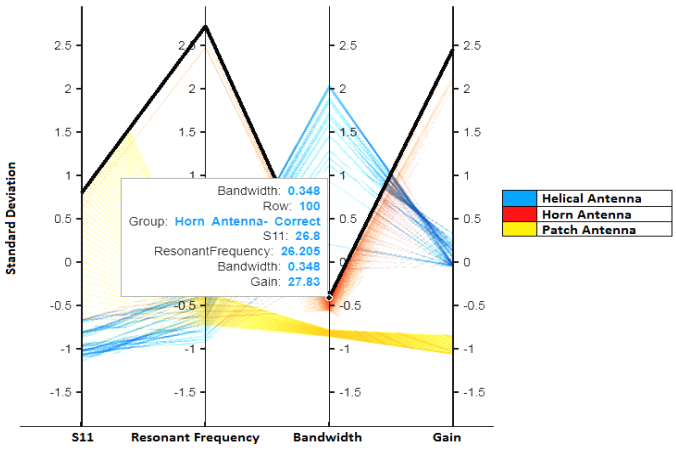

FIGURE 7. Parallel coordinates plot.

"confusion matrix" in academic literature. Figure 6 illustrates the proposed matrix for categorizing antenna confusion. The projected values in each column of the confusion matrix represent the count of predictions made for each class, as denoted by the total number of entries in each column. It is evident that all the numerical values within the diagonal grid have been duly completed, thereby signifying the successful fulfilment of each antenna's designated function. Figure 7 depicts the parallel coordinate's visualization of the antenna dataset. The presented graph depicts the interconnections among input variables, namely resonant frequency (f_r), S_{11}, bandwidth (BW), gain (G), and the standard deviation associated with every class.

The true negative (TN), true positive (TP), false negative (FN), and false positive (FP) values are derived from the confusion matrix. Accuracy, sensitivity, and specificity can then be calculated using Equations (1), (2), and (3), respectively. The experimental findings presented in Table 2 demonstrate that the optimizable KNN algorithm exhibits a significant enhancement in classification speed when being applied to various antenna

TABLE 2. Performance measures of optimizable KNN classifier.

Parameters	Values
Training Time (sec)	14.327
Prediction Speed (observation/sec)	~ 8000
True positive value	40
True negative value	79
False Positive value	1
False Negative value	0
Accuracy (%)	99.16
Sensitivity (%)	100
Specificity (%)	98.75

training set samples. Furthermore, there is potential for further improvement in terms of accuracy, sensitivity, and specificity.

A depiction of the Receiver Operating Characteristic (ROC) curve is shown in Figure 8. The ROC curve provides insight into a classifier's effectiveness. When the classification performance exceeds expectations, the ROC curve approaches unity. Each of the helical antenna, horn antenna, and rectangular patch antenna has a unitary area under its respective curves. The error plot's classification is depicted in Figure 9. The error is zero when the expected value and observed value are identical. Errors are the differences between expected and actual outcomes. When the observed value exceeds the predicted value, the resulting discrepancy is categorised as a positive error.

Partial dependence plot (PDP) illustrates the marginal impact of one or two features on the predicted outcome of a machine learning model. PDP is an effective tool for determining the nature of the correlation between a desired variable and a specified attribute. It can provide insights into whether this relationship is linear, monotonic, or exhibits a more intricate pattern. Partial dependence graphs demonstrate a linear relationship when being employed in the context of a linear regression model.

The probability density function (PDF) of regression is given by

$$g_{s(y_s)} = E_{y_c}\left[g\left(y_s, Y_C\right)\right] = \int g\left(y_s, Y_C\right) dP\left(Y_C\right) \quad (9)$$

The characteristics that should have the PDF drawn are y_s, and the other features employed in the machine learning (ML) model g, which are now considered as random variable, are Y_C. Typically, the set S has just one or two features. S's feature(s) affect prediction; y is the feature space of Y_s and Y_C.

Monte Carlo approach averages training data to estimate partial function g_s:

$$g_s\left(y_s\right) = \frac{1}{n}\sum_{i=1}^{n} g\left(y_s, y_c^{(i)}\right) \quad (10)$$

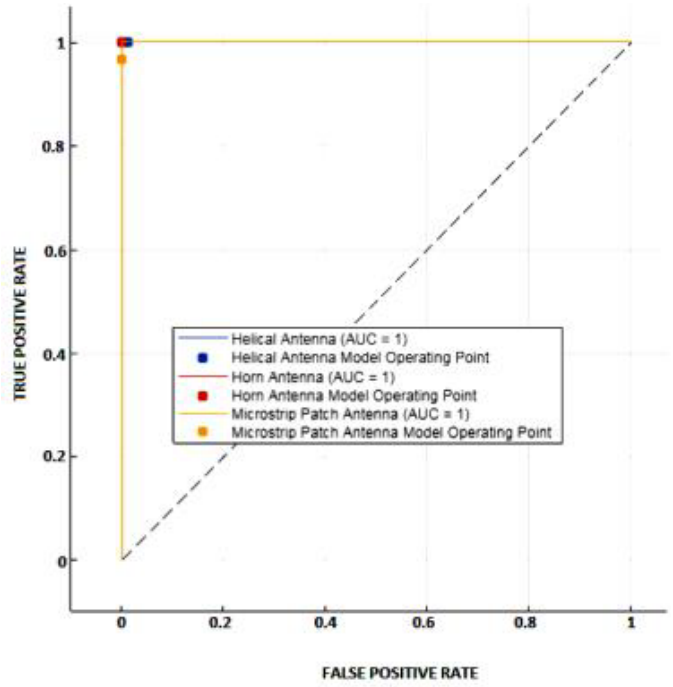

FIGURE 8. ROC curve plot.

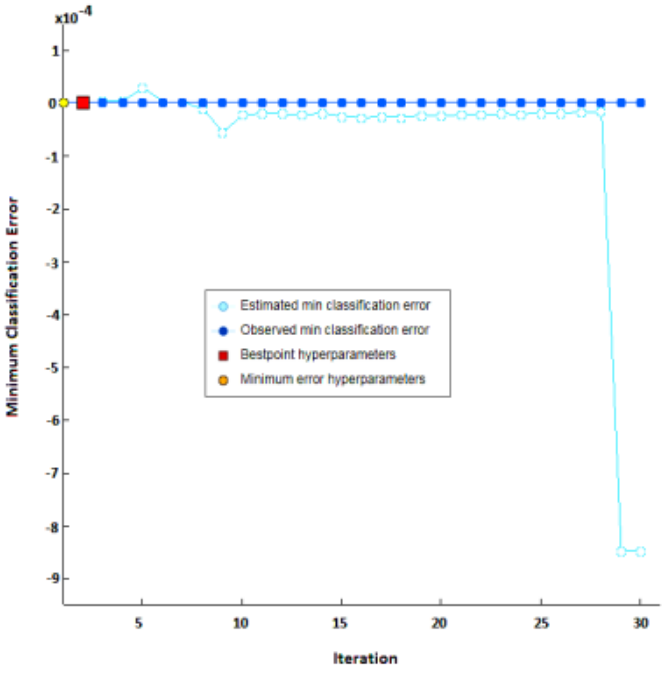

FIGURE 9. Classification error plot.

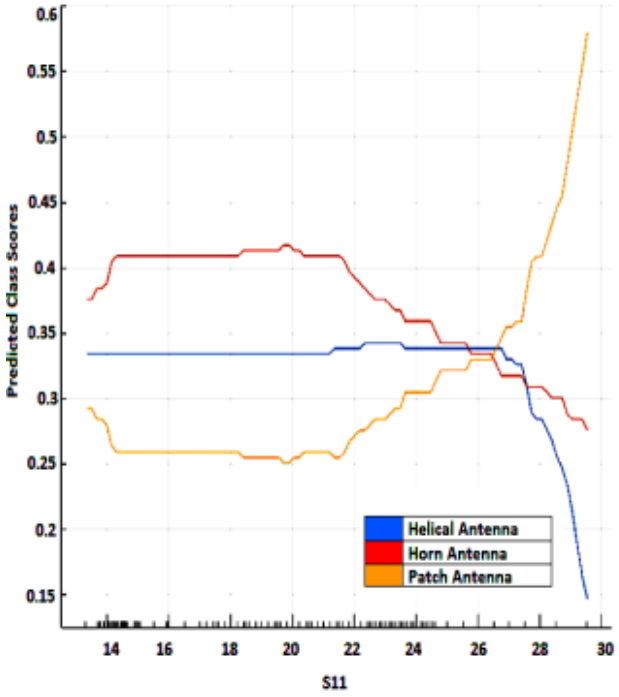

FIGURE 10. PDP for S_{11}.

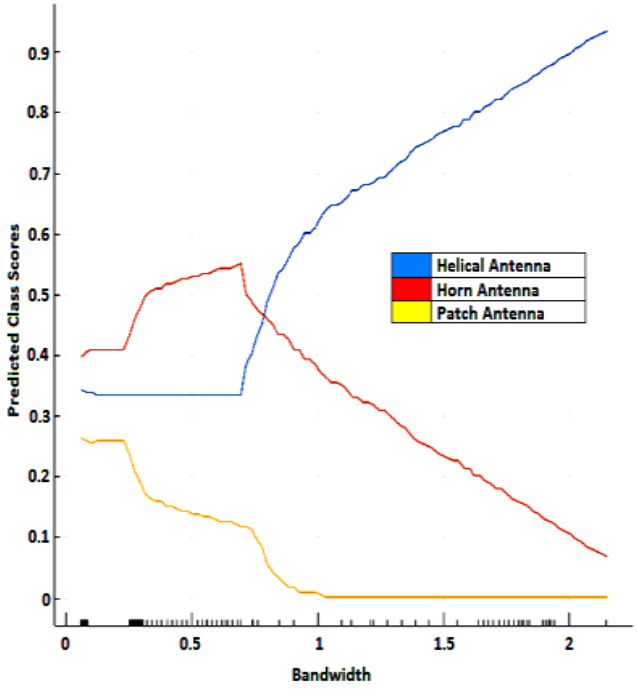

FIGURE 11. PDP for bandwidth.

In this formula, Y_c represents the actual value of a dataset feature, and n represents the number of dataset instances. The PDP presumes no correlation between C and S features.

The information provided by partial dependence plots pertains to the maximal influence of considered features on classification problems. The classification of horn antennas is influenced by the feature resonant frequency and maximal gain, as shown in Figures 12 and 13. Similar to Figure 13 and Figure 11, it is found that gain and bandwidth contributed equally to the classification of helical antennas. The characteristic S_{11} serves a crucial role in the classification of microstrip patch antennas, as shown in Figure 10.

Figure 14 depicts the membership function of the resonant frequency. The resonance frequency of a helical antenna ranges

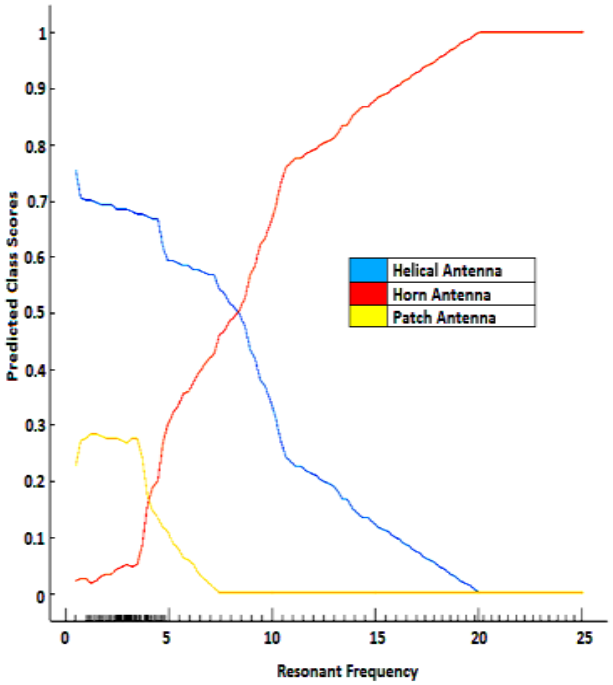

FIGURE 12. PDP for resonant frequency.

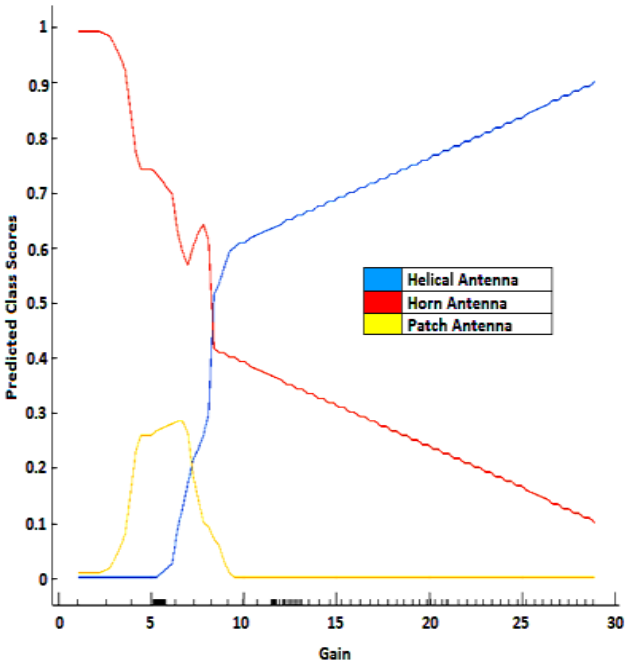

FIGURE 13. PDP for gain.

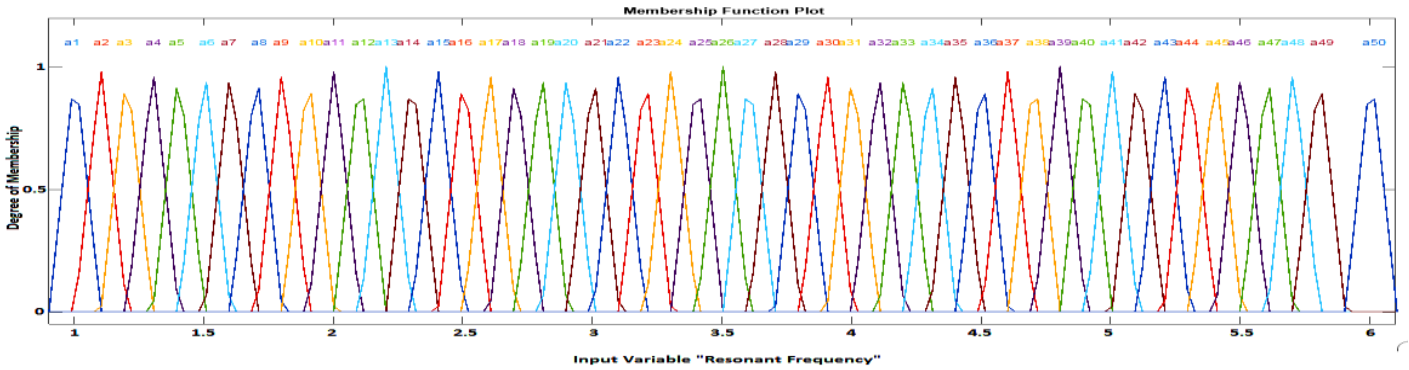

FIGURE 14. Membership function of resonant frequency.

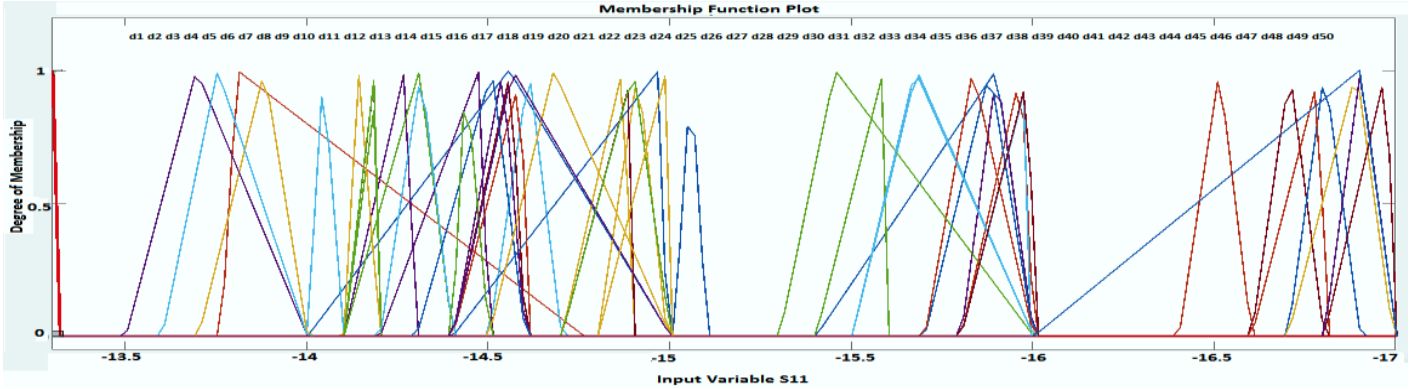

FIGURE 15. Membership function of S_{11}.

from 1 to 6 GHz. Figure 15 depicts the S_{11} membership function. The reflection coefficient ranges from -13 to -17 dB for helical antennas.

Figure 16 depicts the membership function for the helix diameter (a) membership category. In an ANFIS model, the helix diameter is used to define the output membership function. The

TABLE 3. Training and testing error for FIS optimization.

FIS Optimization Method	Width of the Patch Antenna		Helix diameter of helical antenna		Horn diameter of horn antenna	
	Training Error	MAPE	Training Error	MAPE	Training Error	MAPE
Hybrid	2.673×10^{-5}	5.9248×10^{-5}	4.01067×10^{-6}	2.8451	1.5428	1.4514
Back propagation	0.0013875	5.9248×10^{-5}	0.00110813	2.8451	3.8927	1.5827

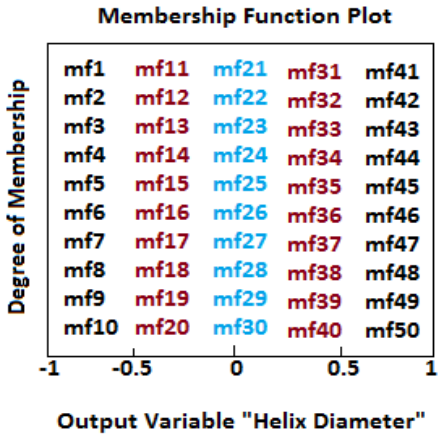

FIGURE 16. Membership function of helix diameter.

S.No	Algorithms	Accuracy
1	Gradient Boosting	91.54%
2	Naive Bayes	94.87%
3	CNN	95.18%
4	SVM	96.84%
5	DT + FIS	99%
6	Proposed Method (Optimizable-KNN+ANFIS)	99.16%

TABLE 4. Performance comparison of proposed method with existing method.

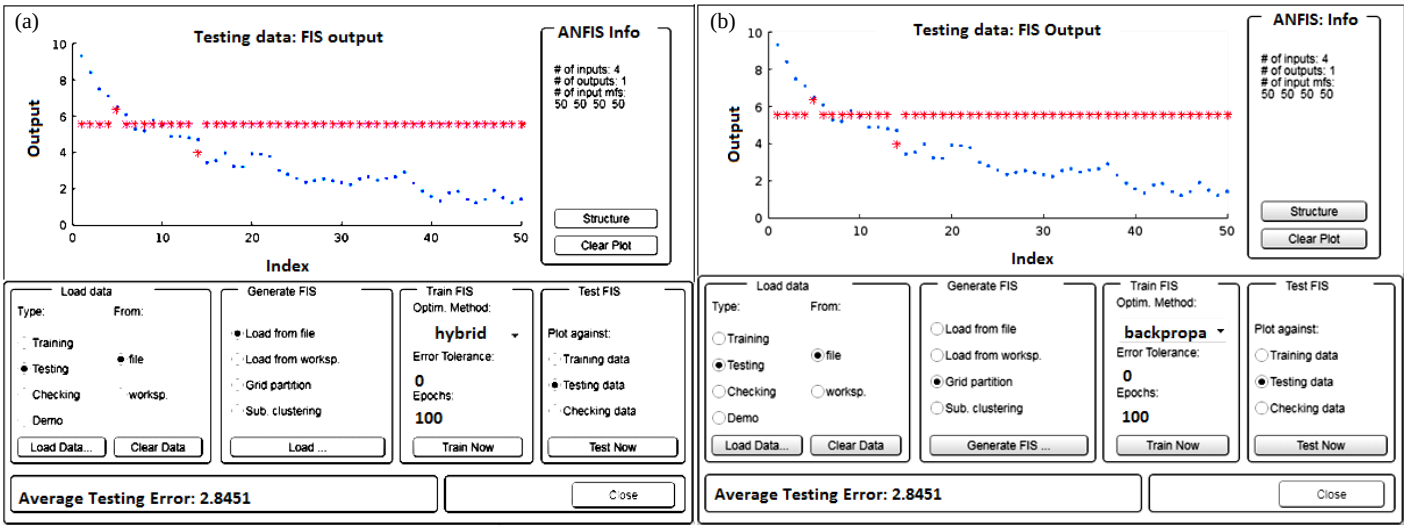

FIGURE 17. (a) ANFIS testing window for parameter prediction of helical antenna when FIS trained using hybrid algorithm. (b) ANFIS testing window for parameter prediction of helical antenna when FIS trained using back propagation algorithm.

triangular membership function is employed in our suggested methodology to analyze different antenna properties. The range of the helix diameter for helical antennas is 1.59 cm to 9.541 cm.

Table 3 displays the training and testing errors associated with the Fuzzy Inference System (FIS) optimization, which incorporates the hybrid and back propagation approach. The training error for hybrid algorithms is found to be smaller in the case of helical antennas than microstrip patch antennas and horn antennas. The hybrid algorithm in microstrip patch antenna exhibits a lower mean absolute percentage error than horn and helical antennas. The training error of the back propagation algorithm is lower in the case of helical antennas than microstrip patch antennas and horn antennas. In contrast to the mean ab-

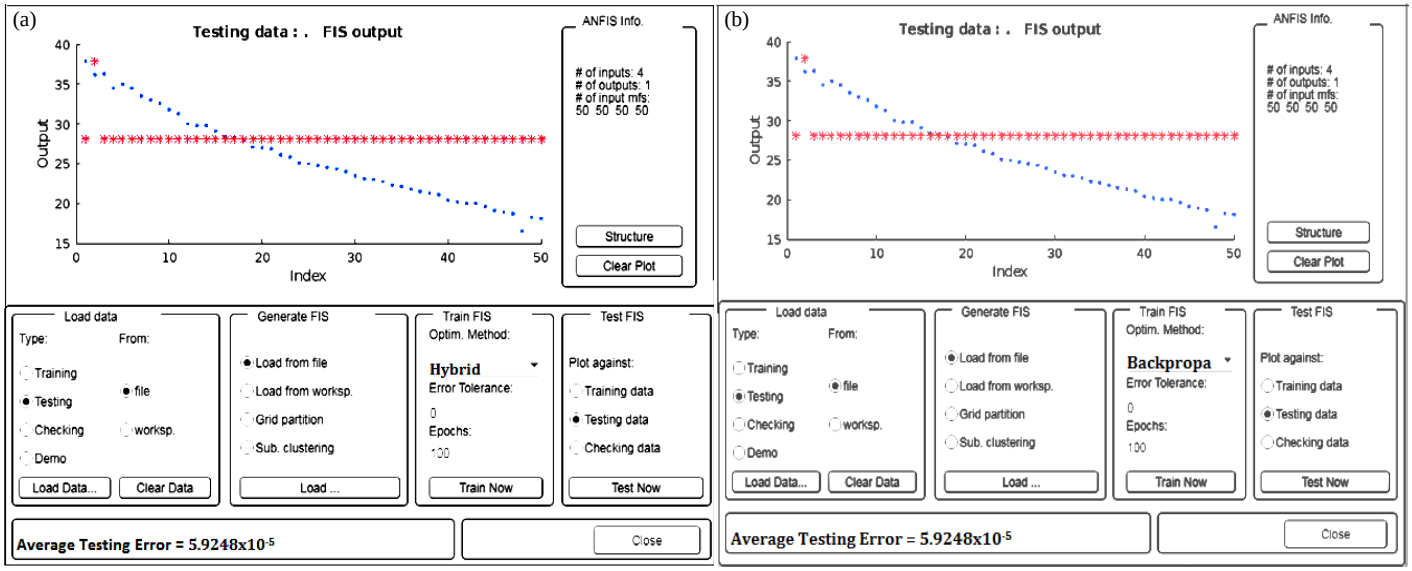

FIGURE 18. (a) ANFIS testing window for parameter prediction of patch antenna when FIS trained using hybrid algorithm. (b) ANFIS testing window for parameter prediction of patch antenna when FIS trained using back propagation algorithm.

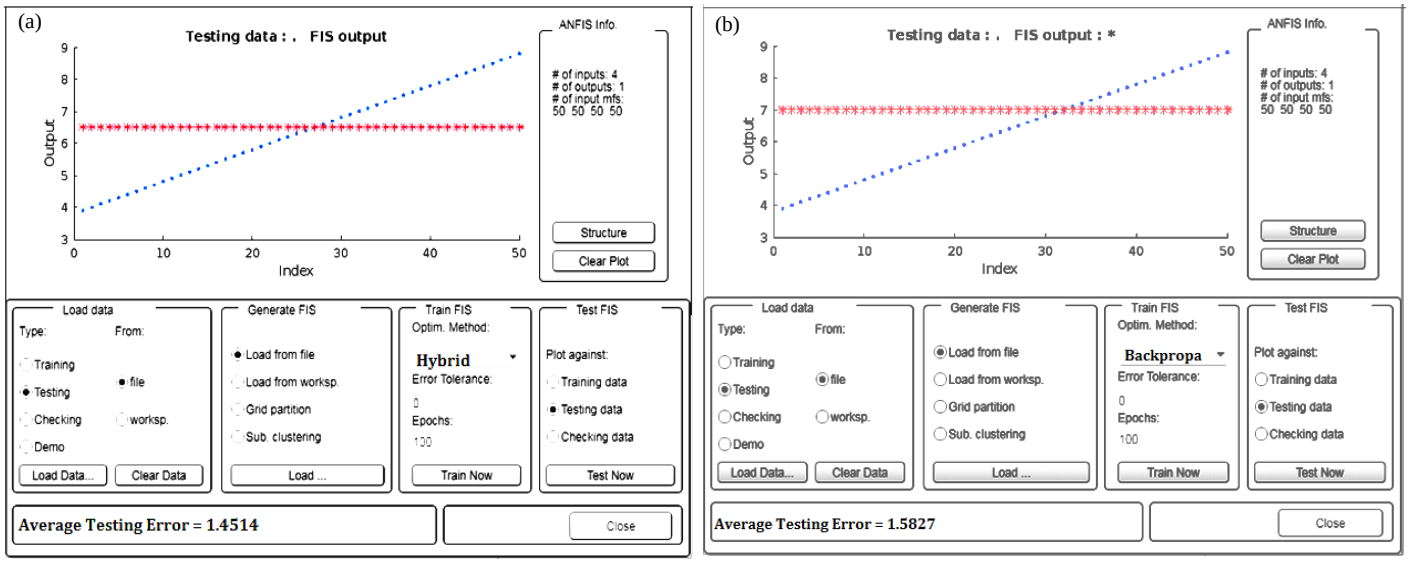

FIGURE 19. (a) ANFIS testing window for parameter prediction of horn antenna when FIS trained using hybrid algorithm. (b) ANFIS testing window for parameter prediction of horn antenna when FIS trained using back propagation algorithm.

solute percentage error (MAPE) exhibited by horn and helical antennas, the MAPE associated with a microstrip patch antenna demonstrates a comparatively reduced value when being utilized in conjunction with the back propagation algorithm.

In Figure 17(a), the ANFIS testing window is depicted, showcasing the prediction of helical antenna parameters when the FIS was trained using a hybrid approach. The initial step involves loading the training data, followed by the establishment of FIS. The ANFIS testing panel will promptly display the training error. In a similar manner, the testing data is loaded, and the FIS is created prior to presenting the average testing error within the ANFIS testing window. The hybrid algorithm yielded an average testing error of 2.8451 for the helical antenna.

The ANFIS testing window for helical antenna parameter prediction is depicted in Figure 17(b), wherein the FIS was trained utilizing a hybrid approach. The initial step involves loading the training data, followed by the establishment of FIS. The ANFIS testing panel will promptly display the training error. In a similar manner, the testing data is loaded and the FIS is created prior to presenting the average testing error within the ANFIS testing window. The average testing error for a helical antenna in the back propagation algorithm is measured to be 2.8451.

The ANFIS testing window for patch antenna parameter prediction is depicted in Figure 18(a), wherein the FIS was trained using a hybrid approach. The initial step involves loading the training data, followed by establishment of FIS. The ANFIS testing panel will promptly display the training error. In a similar manner, the testing data is loaded, and the FIS is created prior to presenting the average testing error within the ANFIS testing window. The hybrid algorithm yielded an average testing error of 5.9248×10^{-5} for the patch antenna. The ANFIS testing window for patch antenna parameter prediction is depicted in Figure 18(b), wherein the FIS was trained using a hybrid approach. The initial step involves loading the training data, followed by establishment of FIS. The ANFIS testing panel will promptly display the training error. In a similar manner, the testing data is loaded, and the FIS is created prior to presenting the average testing error within the ANFIS testing window. The average testing error for a patch antenna in the back propagation algorithm is 5.9248×10^{-5}.

Figure 19(a) illustrates the ANFIS testing window utilized for the prediction of horn antenna parameters, where the FIS was trained using a hybrid approach. The initial step involves loading the training data, followed by the establishment of FIS. The ANFIS testing panel will promptly display the training error. In a similar manner, the testing data is loaded, and the FIS is created prior to presenting the average testing error within the ANFIS testing window. The hybrid algorithm yields an average testing error of 1.4514 for a horn antenna. The ANFIS testing window for horn antenna parameter prediction is depicted in Figure 19(b), wherein the FIS was trained using a hybrid approach. The initial step involves loading the training data, followed by Fuzzy Inference System. The ANFIS testing panel will promptly display the training error. In a similar manner, the testing data is loaded, and the FIS is created prior to presenting the average testing error within the ANFIS testing window. The average testing error for a horn antenna in the back propagation algorithm is measured to be 1.5827.

Table 4 presents a comparative analysis between the proposed system and various machine learning techniques. The results indicate that the suggested methods exhibit greater efficiency than the existing system.

5. CONCLUSION

This research presents the development of an advanced machine learning model that utilizes intelligent algorithms to accurately predict geometric parameters and classify antennas. The proposed model for classifying antennas is based on the ANFIS. The antenna classification model, when utilizing the optimizable KNN classifier, demonstrates a high level of accuracy at 99.16%. Similarly, the model for estimating geometric parameters, employing the adaptive neuro-fuzzy inference system, exhibits a low Mean Absolute Percentage Error of less than 3%. The real-time implementation of the proposed (Optimizable KNN + ANFIS) model is recommended for achieving accurate antenna classification and predicting geometric parameters.

REFERENCES

[1] Pujara, D., A. Modi, N. Pisharody, and J. Mehta, "Predicting the performance of pyramidal and corrugated horn antennas using ANFIS," *IEEE Antennas and Wireless Propagation Letters*, Vol. 13, 293–296, 2014.

[2] Ramasamy, R. and M. A. Bennet, "An efficient antenna parameters estimation using machine learning algorithms," *Progress In Electromagnetics Research C*, Vol. 130, 169–181, 2023.

[3] Kapetanakis, T. N., I. O. Vardiambasis, E. I. Lourakis, and A. Maras, "Applying neuro-fuzzy soft computing techniques to the circular loop antenna radiation problem," *IEEE Antennas and Wireless Propagation Letters*, Vol. 17, No. 9, 1673–1676, Sep. 2018.

[4] Rop, K. V., D. B. O. Konditi, H. A. Ouma, and S. M. Musyoki, "Parameter optimization in design of a rectangular microstrip patch antenna using adaptive neuro-fuzzy inference system technique," *IJTPE Journal*, Vol. 4, No. 3, 16–23, 2012.

[5] Kayabasi, A. and A. Akdagli, "Predicting the resonant frequency of E-shaped compact microstrip antennas by using ANFIS and SVM," *Wireless Personal Communications*, Vol. 82, No. 3, 1893–1906, 2015.

[6] Kayabaşı, A., "Triangular ring patch antenna analysis: Neuro-fuzzy model for estimating of the operating frequency," *The Applied Computational Electromagnetics Society Journal (ACES)*, Vol. 36, No. 11, 1412–1417, 2021.

[7] Sarkar, D., T. Khan, F. A. Talukdar, and Y. M. M. Antar, "Computational intelligence paradigms for UWB antennas: A comprehensive review of analysis, synthesis and optimization," *Artificial Intelligence Review*, Vol. 56, No. 1, 655–684, 2023.

[8] Yahya, S. I., A. Rezaei, and R. I. Yahya, "A new ANFIS-based hybrid method in the design and fabrication of a high-performance novel microstrip diplexer for wireless applications," *Journal of Circuits, Systems and Computers*, Vol. 31, No. 3, 2250050, 2022.

[9] Yiğit, E., "Operating frequency estimation of slot antenna by using adapted kNN algorithm," *International Journal of Intelligent Systems and Applications in Engineering*, Vol. 6, No. 1, 29–32, 2018.

[10] Sachaniya, P. D., J. M. Rathod, and U. Mehta, "Design and fabrication of axially corrugated gaussian profiled horn antenna," *Smart Antennas*, 393–403, Springer, Cham, 2022.

[11] Manshari, S., S. Koziel, and L. Leifsson, "Compact dual-polarized corrugated horn antenna for satellite communications," *IEEE Transactions on Antennas and Propagation*, Vol. 68, No. 7, 5122–5129, 2020.

[12] Hu, C., M. Wei, Y. Zhao, L. Chen, F. Wang, and X. Cao, "A compact normal-mode VHF/UHF dual-band helical antenna for lunar microsatellite," *Aerospace Science and Technology*, Vol. 126, 107584, 2022.

[13] Maged, M., M. El-Telbany, and A. El-Akhdar, "Design optimization for high-gain quad array of helical antennas for satellite applications," in *Recent Advances in Engineering Mathematics and Physics*, 183–190, 2020.

[14] Sadeghikia, F. and A. K. Horestani, "Design guidelines for helicone antennas with improved gain," *Microwave and Optical Technology Letters*, Vol. 61, No. 4, 1016–1021, 2019.

[15] Falkner, B., H. Zhou, and A. Mehta, "A machine learning based traveling wave antenna development methodology," in *2021 IEEE International Symposium on Antennas and Propagation and USNC-URSI Radio Science Meeting (APS/URSI)*, 2040–2041, 2021.

[16] Naderi, S., K. Bundy, T. Whitney, A. Abedi, A. Weiskittel, and A. Contosta, "Sharing wireless spectrum in the forest ecosystems using artificial intelligence and machine learning," *International Journal of Wireless Information Networks*, Vol. 29, No. 3, 257–268, 2022.

[17] Moshtaghzadeh, M., A. Bakhtiari, E. Izadpanahi, and P. Mardanpour, "Artificial neural network for the prediction of fatigue life of a flexible foldable origami antenna with kresling pattern," *Thin-Walled Structures*, Vol. 174, 109160, 2022.

[18] Shi, D., C. Lian, K. Cui, Y. Chen, and X. Liu, "An intelligent antenna synthesis method based on machine learning," *IEEE Transactions on Antennas and Propagation*, Vol. 70, No. 7, 4965–4976, 2022.

[19] Polo-López, L., J. Córcoles, and J. A. Ruiz-Cruz, "Antenna design by means of the fruit fly optimization algorithm," *Electronics*, Vol. 7, No. 1, 3, 2018.

[20] Zhang, X.-Y., Y.-B. Tian, and X. Zheng, "Antenna optimization design based on deep Gaussian process model," *International Journal of Antennas and Propagation*, Vol. 2020, Article ID 2 154 928, 10 pages, 2020.

[21] Mir, F., L. Kouhalvandi, and L. Matekovits, "Deep neural learning based optimization for automated high performance antenna designs," *Scientific Reports*, Vol. 12, No. 1, 16801, 2022.

[22] Almoteriy, M. A., M. I. Sobhy, and J. C. Batchelor, "Characterization of wideband antennas for point-to-point communications," *IEEE Transactions on Antennas and Propagation*, Vol. 66, No. 9, 4466–4473, 2018.

[23] Bradford, E., A. M. Schweidtmann, and A. Lapkin, "Efficient multiobjective optimization employing Gaussian processes, spectral sampling and a genetic algorithm," *Journal of Global Optimization*, Vol. 71, No. 2, 407–438, 2018.

[24] Cui, L., Y. Zhang, R. Zhang, and Q. H. Liu, "A modified efficient KNN method for antenna optimization and design," *IEEE Transactions on Antennas and Propagation*, Vol. 68, No. 10, 6858–6866, 2020.

[25] Jin, J., C. Zhang, F. Feng, W. Na, J. Ma, and Q.-J. Zhang, "Deep neural network technique for high-dimensional microwave modeling and applications to parameter extraction of microwave filters," *IEEE Transactions on Microwave Theory and Techniques*, Vol. 67, No. 10, 4140–4155, 2019.

[26] Elsawy, M. M. R., S. Lanteri, R. Duvigneau, G. Brière, M. S. Mohamed, and P. Genevet, "Global optimization of metasurface designs using statistical learning methods," *Scientific Reports*, Vol. 9, 17918, 2019.

[27] Panagiotou, S. C., S. C. A. Thomopoulos, and C. N. Capsalis, "Genetic algorithms in antennas and smart antennas design overview: Two novel antenna systems for triband GNSS applications and a circular switched parasitic array for wimax applications developments with the use of genetic algorithms," *International Journal of Antennas and Propagation*, Vol. 2014, Article ID 729 208, 13 pages, 2014.

[28] Chou, H.-T., Y.-C. Hou, and W.-J. Liao, "A dual band patch antenna design for WLAN and DSRC applications based on a genetic algorithm optimization," *Electromagnetics*, Vol. 27, No. 5, 253–262, 2007.

[29] Tonn, D. A. and R. Bansal, "Reduction of sidelobe levels in interrupted phased array antennas by means of a genetic algorithm," *International Journal of RF and Microwave Computer-Aided Engineering*, Vol. 17, No. 2, 134–141, 2007.

[30] Varnamkhasti, M. J., L. S. Lee, M. R. A. Bakar, and W. J. Leong, "A genetic algorithm with fuzzy crossover operator and probability," *Advances in Operations Research*, Vol. 2012, Article ID 956 498, 16 pages, 2012.

[31] Aneesh, M., J. Ansari, A. Singh, Kamakshi, and a. S. S. Sayeed, "Analysis of microstrip line feed slot loaded patch antenna using artificial neural network," *Progress In Electromagnetics Research B*, Vol. 58, 35–46, 2014.